Effect of the orientational disorder on the hyperpolarizability measurement of amphiphilic push–pull chromophores in Langmuir–Blodgett monolayers

ARTICLE *in* OPTICS COMMUNICATIONS · MARCH 2005

Impact Factor: 1.45 · DOI: 10.1016/j.optcom.2004.11.057

6 AUTHORS, INCLUDING:

Aymeric Leray
French National Centre for Scientific R…
36 PUBLICATIONS **267** CITATIONS
SEE PROFILE

Yann Le Grand
Université de Bretagne Occidentale
71 PUBLICATIONS **434** CITATIONS
SEE PROFILE

Olivier Mongin
Université de Rennes 1
122 PUBLICATIONS **2,992** CITATIONS
SEE PROFILE

Available online at www.sciencedirect.com
SCIENCE DIRECT®
Optics Communications 247 (2005) 213–223
OPTICS COMMUNICATIONS
www.elsevier.com/locate/optcom

Effect of the orientational disorder on the hyperpolarizability measurement of amphiphilic push-pull chromophores in Langmuir–Blodgett monolayers

A. Leray [a], D. Rouède [a], C. Odin [a], Y. Le Grand [a,*], O. Mongin [b], M. Blanchard-Desce [b]

[a] GMCM, UMR CNRS 6626, Institut de Physique de Rennes, Université de Rennes 1, Campus de Beaulieu, 35042 Rennes, France
[b] SESO, UMR CNRS 6510, Institut de Chimie de Rennes, Université de Rennes1, Campus de Beaulieu, 35042 Rennes, France

Received 15 September 2004; accepted 12 November 2004

Abstract

First-order hyperpolarizabilties of two new amphiphilic push-pull chromophore derivatives of hemicyanine dyes prepared in Langmuir–Blodgett films and designed for membrane potential imaging of living cells are measured by surface second-harmonic generation (SHG). Assuming uniaxial symmetry, an effective hyperpolarizability coefficient β_e is defined, and a procedure to measure this coefficient is described. Relationships between β_e and the true hyperpolarizability coefficient β are derived on the basis of a stochastic model taking account of the tilt angle disorder of the chromophores. Maximum discrepancies between the true and the effective hyperpolarizabilities are calculated as a function of the orientation parameter D, and it is shown that the relative difference may not exceed 40% for usual distribution functions of the tilt angle. As a result, the dominant hyperpolarizability coefficient $\beta^{(2)}_{z,z,z}$ of the chromophores in LB films is found to be in the range $0.3–0.7 \times 10^{-27}$ esu at 1064 nm fundamental wavelength.

PACS: 42.65.Ky; 68.47.Pe
Keywords: Nonlinear optics; Langmuir–Blodgett; Chromophores

1. Introduction

Voltage-sensitive molecular probes play an important role in biological imaging since they act as optical reporters for electrical activity of

* Corresponding author. Tel.: +33 2 23 23 62 11; fax: +33 2 23 23 67 17.
E-mail address: yann.legrand@univ-rennes1.fr (Y.L. Grand).

0030-4018/$ - see front matter © 2004 Elsevier B.V. All rights reserved.
doi:10.1016/j.optcom.2004.11.057

cell membranes [1]. Among these functionalized dyes, nonlinear push-pull chromophores with enhanced quadratic molecular response represented by the hyperpolarizability coefficient β have been recently shown to allow non-invasive recording of fast spatiotemporal modulations of action potentials in living cells via second-harmonic generation (SHG) microscopy [2]. This nonlinear approach based on coherent generation of light from amphiphilic chromophores present in the outer leaflet of cell membranes has proved to be both more sensitive [3,4] and spatially more selective [5] than the corresponding linear one-photon incoherent method based on electrochromism of fluorophores [6–9]. Electric fields associated with transmembrane potentials are indeed strong enough to induce both significant changes of hyperpolarizabilty and realignment of the chromophores [10]. Achievement of the highest molecular hyperpolarizability and electro-optic response is then at the heart of molecular design strategies [11,12], as only low concentrations of markers allow to preserve cell viability over time scales of biological processes and experiments. However, reliable hyperpolarizability measurements of such push-pull molecules are a ticklish problem. Indeed, in situ measurements are rather hazardous due to the lack of control of the marker concentration and organization when incorporated in living cells or in model bilayer lipid membranes. On the other hand, chromophore solutions used for electric-field induced second-harmonic generation (EFISHG) and hyper-Rayleigh scattering (HRS) techniques do not simulate physiological conditions, as it is well known that the solvent environment can greatly modify the optical properties of chromophores [13–15]. In particular, experimental and theoretical studies have shown that both the linear (absorption and emission) and nonlinear optical properties of charged push-pull molecules significantly depend on solvent polarity [16]. Moreover, EFISHG conducted in solution provides only the projection of the dipolar part of the β tensor on the dipole moment μ of the molecules, requiring further measurements of μ as well as local field corrections [13,14] In addition, the third- order polarizability coefficient γ is usually neglected. HRS appears more appropriate since measurement of β is possible without the need of orientating fields [15]. However, in the case of fluorescent chromophores, sophisticated time-resolved setups [17–19] and/or spectral discrimination are needed in order to isolate the weak HRS signal.

Among all possible approaches for measuring hyperpolarizability of functionalized chromophores, surface SHG from molecular monolayers in Langmuir–Blodgett (LB) films present an interesting trade-off between control of parameters (organization, concentration of chromophores, etc.), simulation of membrane environment and experimental suitability. However, although this technique was frequently used to measure the effective orientation of chromophores as well as macroscopic nonlinear susceptibility coefficients of the films [20–25], derivation of the microscopic hyperpolarizability coefficients accounting for the orientational disorder of the molecules has remained an eluded question up to now. The aim of this paper is to address this problem in the frame of surface SHG measurements of two functionalized push-pull chromophores deposited in LB monolayers and designed for membrane potential imaging [2,10,26].

2. Theory and methodology

The hyperpolarizability tensor of push-pull chromophores is usually dominated by a single axial coefficient $\beta^{(2)}_{z,z,z} \equiv \beta$ associated with the push-pull molecular axis z. To quantify β from SHG measurements on LB monolayers, the hyperpolarizabilty tensor of the individual molecule has to be related to the macroscopic susceptibility tensor of the film through summation over all possible orientations of the molecules in the monolayer. In case where isotropic orientation distribution about the normal axis Z of the film is assumed (condition easily verified from cancellation of SHG at normal incidence on the film), that is a random azimuth of the molecules within the monolayer plane (see Fig. 1), the two non-vanishing independent elements of the surface macroscopic susceptibility tensor $\chi^{(2)}$ are given by [21]

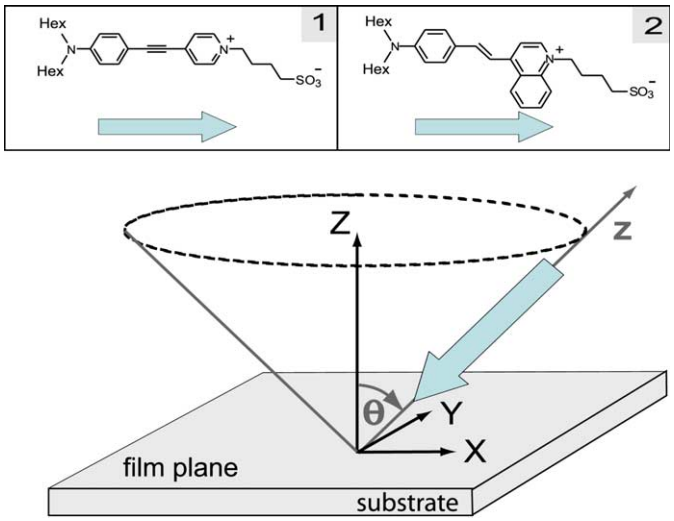

Fig. 1. Model of random azimuthal orientation of the dye molecules in the LB film. θ is the angle between the surface normal laboratory axis Z and the aromatic molecular axis z active in SHG, which is supposed to be almost parallel to the principal axis corresponding to $\beta^{(2)}_{z,z,z}$. The molecular structures of the two zwitterionic amphiphilic push-pull chromophores 1 and 2 under study are represented in the inset.

$$\chi_{33} = N_s\beta\langle\cos^3\theta\rangle, \quad \chi_{15} = \frac{1}{2}N_s\beta\langle\cos\theta\sin^2\theta\rangle = \frac{1}{2}N_s\beta(\langle\cos\theta\rangle - \langle\cos^3\theta\rangle), \tag{1}$$

using the usual index contraction for the elements of $\chi^{(2)}$ [27], and neglecting any correction for local field effects [22].

In Eq. (1), N_s is the surface density of active chromophores (molecules/m^2) and the tilt angle θ is the angle between the principal axis z associated with $\beta_{z,z,z}$ and the interface normal axis Z (see Fig. 1). The brackets $\langle\,\rangle$ indicates an average over the molecular orientation which has to be weighted by the orientational distribution function $w(\theta)$, in such a way that

$$\langle\cos^n\theta\rangle = \frac{\int_0^\pi \cos^n\theta w(\theta)\sin\theta\,\mathrm{d}\theta}{\int_0^\pi w(\theta)\sin\theta\,\mathrm{d}\theta}, \tag{2}$$

where the $\sin\theta$ term accounts for the metrics of the spherical coordinates. The ratio χ_{33}/χ_{15} can be derived by fitting the SHG intensity measured as function of the input polarization [25]. Expressions of the saggital (s) and parallel (p)-polarized second-harmonic (at frequency 2ω) responses $I^{2\omega}_{s,p}$ of a thin slab (much thinner than a wavelength) of nonlinear material as function of the input fundamental intensity I^ω (at frequency ω) have been derived analytically [24]. These expressions can be written in the following condensed form:

$$I^{2\omega}_{s,p} = \frac{128\pi^3\omega^2\chi^2_{15}F^2_{s,p}(I^\omega)^2}{c^3}, \tag{3}$$

using the factor $F_{s,p}$ which accounts for all the linear and nonlinear refractive processes at the different interfaces. Owing to the microscopic and macroscopic uniaxial symmetries of the molecular monolayer considered here, $F_{s,p}$ can be written as [24,25]

$$F_s = |a_1\sin 2\gamma|,$$
$$F_p = |a_2\cos^2\gamma + a_3\sin^2\gamma + (\chi_{33}/\chi_{15})a_4\cos^2\gamma|, \tag{4}$$

where γ stands for the polarization angle of the pumping field with respect to the plane of incidence (see Fig. 2), and a_i are coefficients which hold for the linear and nonlinear Fresnel coefficients at the different interfaces (see Appendix A). While F_s relies on the coefficients a_i, on γ and on the angle of incidence, F_p depends further on the ratio χ_{33}/χ_{15}. This ratio can be derived by fitting the p-polarized component of the SHG intensity measured as

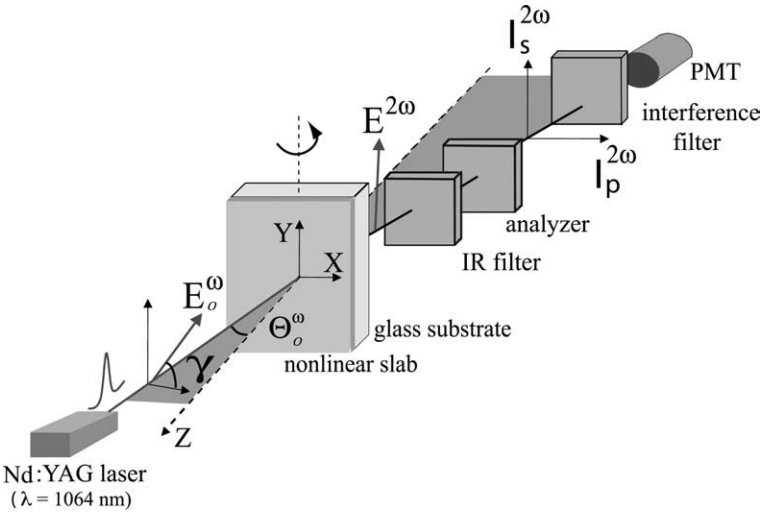

Fig. 2. Schematic of the experiment. The direction of polarization γ of the incident pumping field $\mathbf{E}_o^{\omega}$ from the picosecond Nd:YAG laser source was controlled with a half-wave plate (not represented). The glass substrate was rotated about the Y-axis up to the incident angle Θ_o of 70°. The transmitted SHG intensities $I_p^{2\omega}$ and $I_s^{2\omega}$ were measured as a function of γ for, respectively, the p (parallel to the X-axis) and s (parallel to the Y-axis) directions of the analyzer. The filters were composed of a high density (ND10) infrared filter and of a narrow band interference filter at $\lambda = 532$ nm , PMT: photomultiplier tube.

function of γ with the expression of F_p^2, at a given angle of incidence [25,28].

An *orientation parameter* D and subsequently an effective (or apparent) molecular orientation angle θ_e are usually defined from this ratio through the following expression [29]:

$$D = \frac{\langle \cos^3\theta \rangle}{\langle \cos\theta \rangle} = \frac{\chi_{33}/\chi_{15}}{2 + \chi_{33}/\chi_{15}} = \cos^2\theta_e. \tag{5}$$

It is clear from Eq. (5) that the effective angle θ_e merges into the angle of maximum probability θ_o as the distribution function $w(\theta)$ sharpens. Otherwise, the maximum discrepancy between θ_e and θ_o depends on the value of D, and on the magnitude of disorder [28].

An effective hyperpolarizability coefficient β_e can be similarly defined by rewriting Eq. (1) as follows [28]:

$$\chi_{33} = N_s\beta_e\cos^3\theta_e = N_s\beta_e D^{3/2},$$
$$\chi_{15} = \frac{N_s\beta_e}{2}\cos\theta_e\sin^2\theta_e = \frac{N_s\beta_e}{2}D^{1/2}(1-D). \tag{6}$$

The surface density of chromophores N_s can be known from measuring the surface area A per molecule in the LB monolayer ($N_s = A^{-1}$). Thus, provided that χ_{33} or χ_{15} can be measured in the absolute, for instance by comparison with a reference nonlinear material (see Appendix B), the effective hyperpolarizability coefficient β_e can be quantified. Then a combination of Eqs. (1) and (6) leads to the following meaningful relationship between β_e and β:

$$\frac{\beta_e}{\beta} = \sqrt{\frac{\langle \cos\theta \rangle^3}{\langle \cos^3\theta \rangle}} = \frac{\langle \cos\theta \rangle_D}{\sqrt{D}}, \tag{7}$$

where $\langle\ \rangle_D$ means that the average is calculated at given D. As shown by Eq. (7), β_e corresponds directly to β for a sharply peaked distribution function $w(\theta)$. However, more or less disagreement between these two coefficients β_e and β is expected according to the magnitude of the tilt angle disorder. The discrepancy between β_e and β cannot be derived from Eq. (7) since the average quantities $\langle \cos\theta \rangle$ and $\langle \cos^3\theta \rangle$ are not measurable separately. However, although the true hyperpolarizability coefficient β remains inaccessible to any investigation limited to surface SHG experiments, we will show in the following that the only knowledge of D sets quite restricted bounds to possible values of β.

3. Material and experiment

The two molecules considered in the present study (see Fig. 1) were prepared using Wittig and Sonogashira coupling reactions [30]. These zwitterionic compounds are amphiphilic derivatives [11] of hemicyanine dyes, which are functionalized to act as nonlinear membrane markers. The push-pull structure provides the molecular asymmetry and potentially large first-order hyperpolarizability. In addition, by grafting hydrophobic chains on the electron-releasing end-group and by using zwitterionic electron-withdrawing moieties, amphiphilic derivatives are obtained. This should favor asymmetrical incorporation in the lipid monolayer, thus ensuring the non-centrosymmetry required for SHG. The dyes were dissolved in R.P. Normapur™ 99–99.4% chloroform at a concentration equal to 0.5×10^{-3} mol/L. LB depositions were obtained by means of a computer-controlled LB Teflon trough (Nima model 112) under surface pressure control (Nima surface pressure sensor, PS4). The LB setup was completed by a Nima dipper mechanism D1L for the deposition. Details of the protocol we used for depositing the films are reported elsewhere [28]. In summary, monolayers were compressed to the desired surface pressure of 35 mN/m, which corresponds to a mean molecular area A of 49 and 38 Å^2 and to a surface density of chromophores $N_s = 1/A$ of, respectively, 2.0×10^{18} and 2.6×10^{18} m^{-2} for compounds 1 and 2, respectively. After an appropriate equilibration period, the films were transferred onto microscope glass slides while maintaining a constant surface pressure.

The experimental setup for SHG measurements is reported in Fig. 2. The laser source was a picosecond Q-switched mode-locked flash-pumped Nd:YAG laser (Quantel France, YG501) emitting on its fundamental infrared wavelength of $\lambda = 1064$ nm. The laser turned out 35 ps pulses at a repetition rate of 20 Hz, with a maximum energy per pulse up to 30 mJ. In fact, the energy was reduced to about 1 mJ to avoid any optical damage of the films. The laser beam was then passed through a set of a fixed polarizer (not represented) followed by a rotating half-wave plate in order to turn the input polarization from the X (parallel to the plane of incidence p) to the Y (normal to the plane of incidence s) axes within a precision of about $\frac{1}{2}^\circ$.

The IR beam was moderately focused (lens not represented) towards the samples which were placed in extrafocus position where the transverse spot size was of about 5 mm. The transmitted intensity from the LB film was passed through a high density IR filter (ND10) followed by a narrow band interference filter centered on 532 nm so as to reject all the infrared photons. The second-harmonic signal produced by the film was then analyzed with a rotating analyzer, oriented either along the X or the Y axis. Finally, the signal was detected with a 600 ps rise time photomultiplier tube (Hamamatsu PMT, H5783-01) connected to the 50 Ω input impedance of a fast 2.5 Gs/s digital oscilloscope (Tektronix, TDS 620B) used as a sampler and averager (over 200 laser pulses). The films were positioned on a rotation stage in order to adjust the angle of incidence Θ_o^ω and were always irradiated with the nonlinear slab facing towards the incident IR pump beam. SHG intensity from LB films was measured as function of the angle of polarization γ of the input electric field $\mathbf{E}_o^\omega$ relatively to the XZ plane of incidence. Θ_o^ω was always kept constant at 70°, since it corresponds to the maximum of the a_4 coefficient in Eq. (4), leading to the best precision in measurement of the ratio χ_{33}/χ_{15} using this method [24].

4. Results

The p and s components of the SHG intensity drawn as a function of the input polarization for the LB films of the two compounds are shown in Fig. 3. The dots account for the experimental data while the full lines are the best fits obtained from Eq. (4). The fitting procedure requires at first to determine the Fresnel coefficients involved in Eq. (4) (see Appendix A). These coefficients depend on the incidence angle Θ_o^ω in air, on the refractive indices n_s^ω and $n_s^{2\omega}$ of the nonlinear slab (the monolayer) and on those $n_g^{2\omega}$ of the glass substrate. The value of $n_g^{2\omega}$ was found to be 1.513 at $\lambda = 589$ nm using a Pulfrich refractometer, then extrapolated to 1.515 at $\lambda = 532$ nm from standard dispersion

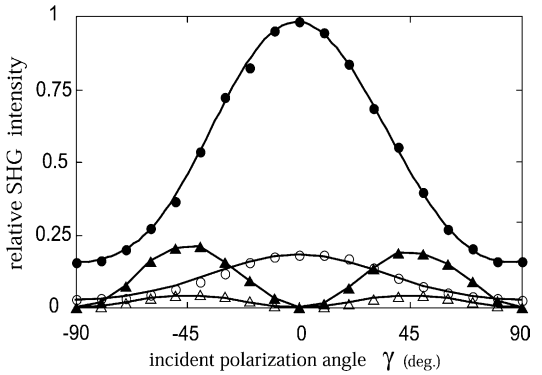

Fig. 3. Polarization dependence of the $I_p^{2\omega}$ (circles) and $I_s^{2\omega}$ (triangles) SHG intensity measured from LB films realized from compounds 1 (open dots) and 2 (solid dots) for an incidence angle $\Theta_o^{\omega} = 70°$. The full lines correspond to the best fits obtained from Eq. (4).

formula for glass. Moreover, n_s^{ω} or $n_s^{2\omega}$ cannot be measured by usual linear optical methods due to the fineness of monolayers (≈1 nm). However, such a small thickness allows us to neglect dispersion on n_s when fitting SHG data ($n_s^{\omega} \approx n_s^{2\omega}$) [24]. Then a unique value of n_s can be obtained in a quite straightforward manner using the fact that peculiar ratios of cross-polarized SHG intensities, say $I_s^{2\omega}(\gamma = 45°)/I_p^{2\omega}(\gamma = 90°)$, are independent of the nonlinear susceptibility coefficients of the film. A more precise procedure to determine n_s, χ_{33}/χ_{15}, D (and θ_e) consists in fitting simultaneously $I_s^{2\omega}(\gamma)$ and $I_p^{2\omega}(\gamma)$ with a least square minimization procedure such as the simplex search method for instance [31]. Using this method, we found $n_s = 1.54$ and 1.43, $\chi_{33}/\chi_{15} = 1.4$ and 1.6, $D = 0.41$ and 0.45 and $\theta_e = 51°$ and 48° for compounds 1 and 2, respectively. Moreover, the overall agreement between data and fits (see Fig. 3) supports well our starting assumptions, say a dominant hyperpolarizability component β_{zzz} with a random azimuth of the chromophores. Discussion of values found for the effective angle θ_e on the basis of the molecular organization in the monolayer is reported elsewhere [28].

As explained in the previous chapter, determination of the effective hyperpolarizability of the chromophores requires absolute measurements of the nonlinear coefficients χ_{15} and/or χ_{33} (at a given D), which can be done by comparison with a reference crystal such as quartz. Here, the nonlinear susceptibility component χ_{15} of the LB film was estimated relatively to the $\chi_{11q} = 1.9 \times 10^{-9}$ esu [32] coefficient of a $l = 4$ mm thick Y-cut quartz plate using the Maker fringe method (see Appendix B). Using this method we found that $\chi_{15} = 1.2 \times 10^{-14}$ and 2.5×10^{-14} esu for compounds 1 and 2, respectively. Then, from Eq. (6), we finally obtained $\beta_e = 0.3 \times 10^{-27}$ esu for compound 1 and 0.5×10^{-27} esu for compound 2.

5. Discussion

Prior to quantify the effect of orientational disorder on the discrepancy between the true hyperpolarizability coefficient β and the effective measured one β_e, the following statements have to be pointed out. Firstly, in the present work, the functionalized amphiphilic molecules are deposited as monolayers on substrates whose surface has hydrophilic affinity. Therefore, the probability for a chromophore to be oriented such that the tilt angle $\theta \geqslant \pi/2$ is negligible (i.e. $w(\theta) = 0$ for $\theta > \pi/2$). Under this statement, it can be shown from Jensen's inequalities [33] that β_e always underestimates β ($\beta_e/\beta \leqslant 1$), whatever the distribution function $w(\theta)$ (over $[0,\pi/2]$). As shown by Eq. (7), the upper bound of β_e/β ($\beta_e/\beta = 1$) corresponds obviously to the δ-distribution. Secondly, since the determination of the lower bound of β_e/β as function of the orientation parameter D cannot be generalized to any distribution function $w(\theta)$, our analysis is limited to some usual distributions.

The gaussian function $w(\theta) \sim \exp(-(\theta - \theta_o)^2/2\sigma^2)$ is often considered as it is the most familiar two-parameter probability density. Strictly speaking, two cases should be distinguished since the gaussian distribution is mostly suited for unlimited variables on the line $[-\infty +\infty]$. On the one hand, if $0 < \theta_o - 3.5\sigma < \theta_o + 3.5\sigma < \pi/2$, then approximatively 99.95% of the probability is confined within $[0,\pi/2]$, and the two parameters θ_o and σ correspond with a good accuracy to their usual meaning, that is the mean tilt angle and angular dispersion, respectively. On the other hand, when the bounds defined above are not satisfied, then the gaussian function has to be wrapped [29] or

truncated to the interval of study [0,π/2]. In that case no more simple relationship between the true mean and dispersion as a function of θ_o and σ can be found, so that a numerical analysis has to be performed.

The lower bounds of β_e/β were sought for two different angular distributions $w(\theta)$ (see Fig. 4): (i) a gaussian truncated over [0,π/2], which was studied numerically, and (ii) a uniform distribution which gave analytical expressions presented in detail in the following. Results that correspond to the wrapped gaussian are not reported here since they were very similar to those obtained for the truncated gaussian, suggesting that our model may be quite representative of a general behavior.

The two-parameter uniform distribution can be characterized by its center θ_o and width δ, such that $0 \leqslant \theta_o - \delta/2 \leqslant \theta_o + \delta/2 \leqslant \pi/2$. Note that, by setting $\theta_o - \delta/2 = 0$, this distribution reduces to the usual conical one where the main molecular axis is uniformly distributed within a cone of half-angle δ. By integration of Eq. (2) for $n = 1$ and 3, we obtained the orientational parameter D, whose definition is given by Eq. (5) as follows:

$$D(\delta,\theta_o) = \frac{1}{2}(1 + \cos\delta\cos 2\theta_o). \tag{8}$$

This formula gives a relationship between δ and θ_o at given D. It is worthwhile to note that $D = 1/2$ if $\delta = \pi/2$ (uniform distribution over [0,π/2]) or $\theta_o = \pi/4$ whatever the angular disorder δ. Since θ belongs to the interval [0,π/2], the parameters δ and θ_o are bounded in order to keep the shape of the uniform distribution constant: (1) for θ_o within [0,π/4], $0 \leqslant \delta \leqslant 2\theta_o$; (2) for θ_o within [π/4,π/2], $0 \leqslant \delta \leqslant \pi - 2\theta_o$. At given D, Eq. (8) shows that these bounds are equivalent to

$$\sqrt{|2D-1|} \leqslant \cos\delta \leqslant 1 \tag{9}$$

Combining Eqs. (2) and (8) provides us with an expression of $\langle\cos\theta\rangle_D$ at fixed D, which gives from Eq. (7)

$$\frac{\beta_e}{\beta} = \frac{1}{2\sqrt{D}}\sqrt{(1+\cos\delta)\left(1+\frac{2D-1}{\cos\delta}\right)}. \tag{10}$$

Then the lower bound of β_e/β, say $\mathrm{Min}(\beta_e/\beta)$, was obtained by substituting in Eq. (10) the lower bound of $\cos\delta$ given by Eq. (9). For $0 \leqslant D \leqslant 1/2$, we found that $\mathrm{Min}(\beta_e/\beta) = 1/\sqrt{2}$, independently to D, whereas for $1/2 \leqslant D \leqslant 1$ the lower bound can be written as $(1+\sqrt{2D-1})/2\sqrt{D}$. By using the upper bound of $\cos\delta$, we recovered in a similar way the corresponding maximum of β_e/β, that is $\mathrm{Max}(\beta_e/\beta) = 1$. For the truncated gaussian distribution, the lower bound of β_e/β was evaluated numerically with the following method. The values of $D(\theta_o,\sigma)$ were calculated on a fine grid of θ_o and σ, which were varied by step of 1° from 2° to 90°. Then, for each D value of interest, all the couples of values $(\theta_o(D),\sigma(D))$ consistent with this D value were extracted, and $\mathrm{Min}(\beta_e/\beta)$ was estimated.

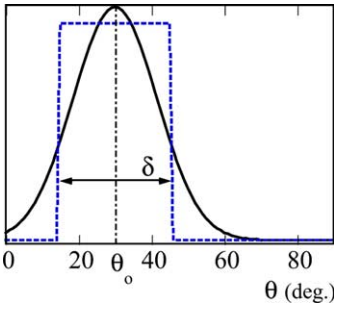

Fig. 4. Orientational distribution functions used in this work. Dotted line: uniform distribution function of mean orientation angle $\theta_o = 30°$ and width $\delta = 30°$. Continuous line: truncated gaussian of mean orientation angle $\theta_o = 30°$ and dispersion $\sigma = 8.66°$. The two distributions are normalized and have the same centered second moments. The tilt angle is restricted to [0,π/2] for amphiphilic monolayers.

Fig. 5 reports the relative maximum discrepancy $\Delta\beta/\beta = \mathrm{Min}[(\beta_e - \beta)/\beta]$ for the two distribution functions. This discrepancy, which is found to be a decreasing function of D, determines the uncertainty on β associated to the lack of knowledge on the chromophore organization within the monolayer. For the uniform distribution, the maximum relative discrepancy is roughly $\Delta\beta/\beta \approx -30\%$ for $D < 1/2$, and smaller for $D > 1/2$. At a given D, the value of $\Delta\beta/\beta$ numerically found for the truncated gaussian is always larger than those of the uniform distribution. For $D < 0.2$, in which case the chromophore principal axis is almost parallel to the supporting surface, $\Delta\beta/\beta$ is about −40% for the truncated gaussian. This difference in behavior could be explained by the higher flexibility of the truncated gaussian compared to

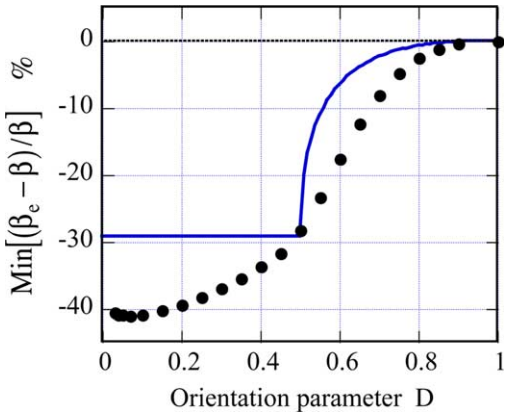

Fig. 5. Maximum relative discrepancy in % between the true hyperpolarizability coefficient β and the estimated hyperpolarizability coefficient β_e, $\Delta\beta/\beta = \mathrm{Min}[(\beta_e - \beta)/\beta]$, as a function of D. Continuous lines (-): analytical results for the uniform distribution. (•): numerical results for the truncated gaussian.

the uniform distribution, the width of this latter being constrained by Eq. (9). In all cases, when the chromophore principal axis is closed to the normal of the film, say for $D > 0.7$, $\Delta\beta/\beta$ is less than -10%, insuring a high reliability of the surface SHG method for measuring β from β_e.

Considering the values of D found for compounds 1 and 2 ($D \approx 0.41$–0.45), the underestimation of β is expected to be no more than 35% whatever the tilt angle distribution function considered. From the measured values of β_e reported in Section 4, we then found $0.3 \leqslant \beta \leqslant 0.5 \times 10^{-27}$ esu and $0.5 \leqslant \beta \leqslant 0.7 \times 10^{-27}$ esu at 1064 nm fundamental wavelength for compounds 1 and 2, respectively. The uncertainty on β as inferred from β_e is within the overall experimental error of our SHG measurements. Moreover, such values are quite comparable with those of other hemicyanines [34] measured by EFISHG or HRS, bringing proof that these chromophores are potentially good candidates for SHG microscopy of membranes in the near IR.

6. Conclusion

The macroscopic as well as the microscopic nonlinear optical properties of two new amphiphilic push-pull chromopores designed for membrane potential imaging have been addressed by means of polarization dependent surface SHG measurements performed on Langmuir–Blodgett monolayer films. An effective hyperpolarizability coefficient β_e of the molecules has been introduced, then measured by calibration of the SHG signals against a reference nonlinear crystal.

Relationships between β_e and the true hyperpolarizability coefficient β have been derived on the basis of a stochastic model where the tilt angle of chromophores was assumed to be limited to the interval $[0,\pi/2]$ and dispersed according to uniform truncated gaussian distribution functions. Within these assumptions, this model has shown for the first time to our knowledge that (i) bounds on β can be obtained from the sole measurements of β_e and of the orientation parameter D, (ii) β_e always underestimated β, (iii) the maximum deviation between the true and the effective (or apparent) hyperpolarizabilities was limited to about 40% in the worse case.

This contribution to the uncertainty on the determination of β is of the order of the overall precision of any of the methods used to measure quadratic hyperpolarizabilities, showing us that surface SHG on Langmuir–Blodgett monolayers is a reliable and easy to implement technique for measuring the microscopic nonlinear optical properties of functionalized chromophores.

Acknowledgment

We gratefully acknowledge financial support from Région Bretagne and Rennes Métropole.

Appendix A

The theoretical interpretation of the SHG intensity generated by a thin nonlinear slab sandwiched between two linear dielectric substrates was first due to Bloembergen and Pershan [35] in the early '60s. In this important work the authors gave a complete description of the interaction process between the ω and 2ω waves in the slab and they solved the Maxwell's equations in order to extract the second harmonic electric field generated by the

nonlinear medium. Later, several authors [23–25,36–38] gave the expression of the SHG intensity generated by the slab taking account of the corrections due to the refractive processes of the ω and 2ω waves at the interfaces between the slab and the substrates. In the present case of the slab/glass transmission geometry, the SHG intensity given by Eq. (3) and the expression of the coefficients a_i involved in this equation can be found in Dick et al. [24]

$$\begin{aligned} a_1 &= f_s^{2\omega} f_Y f_Z \tilde{f}_Y \sin\Theta_o^\omega, \\ a_2 &= f_p^{2\omega}(f_X f_Z \tilde{f}_X \sin 2\Theta_o^\omega + f_X^2 \tilde{f}_Z \cos^2\Theta_o^\omega), \\ a_3 &= f_p^{2\omega} f_Y^2 \tilde{f}_Z, \\ a_4 &= f_p^{2\omega} f_Z^2 \tilde{f}_Z \sin^2\Theta_o^\omega. \end{aligned} \tag{A.1}$$

In this equation f, $\tilde{f}$ and $f^{2\omega}$ are factors which describe refraction of the ω and 2ω waves at the different interfaces, and Θ_o^ω is the angle of incidence of the input beam at the air/slab interface (see Fig. 6).

In summary, factors f which describe linear refraction of the input beam at the air/slab interface and are given by the following expressions [39]:

$$\begin{aligned} f_X &= \frac{2\ \sin\Theta_s^\omega\ \cos\Theta_s^\omega}{\sin(\Theta_o^\omega + \Theta_s^\omega)\ \cos(\Theta_o^\omega - \Theta_s^\omega)}, \\ f_Y &= \frac{2\sin\Theta_s^\omega \cos\Theta_o^\omega}{\sin(\Theta_o^\omega + \Theta_s^\omega)}, \\ f_Z &= \frac{2\sin\Theta_s^\omega \cos\Theta_o^\omega}{n_s^\omega \sin(\Theta_o^\omega + \Theta_s^\omega)\ \cos(\Theta_o^\omega - \Theta_s^\omega)}, \end{aligned} \tag{A.2}$$

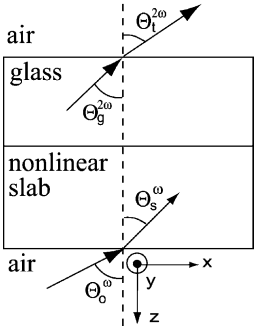

Fig. 6. Schematic diagram describing the propagation of the fundamental ω and harmonic 2ω waves in the LB film. Θ_o^ω, Θ_s^ω and $\Theta_g^{2\omega}$, $\Theta_t^{2\omega}$ are the angles of incidence and refraction for the ω and 2ω waves at the air/slab and glass/air interfaces, respectively.

where Θ_s^ω is the angle of refraction of the input beam at the air/slab interface (see Fig. 6), and n_s^ω is the refractive index of the slab at ω. Coefficients $\tilde{f}$, describing the nonlinear refraction of the 2ω wave at the slab/glass interface, are given by [24]

$$\begin{aligned} \tilde{f}_X &= \frac{\cos\Theta_o^\omega \sin\Theta_g^{2\omega}}{\cos(\Theta_g^{2\omega} - \Theta_o^\omega)\sin(\Theta_o^\omega + \Theta_g^{2\omega})}, \\ \tilde{f}_Y &= \frac{\sin\Theta_g^{2\omega}}{\sin(\Theta_o^\omega + \Theta_g^{2\omega})}, \\ \tilde{f}_Z &= \frac{\sin\Theta_o^\omega \sin\Theta_g^{2\omega}}{(n_s^{2\omega})^2 \cos(\Theta_g^{2\omega} - \Theta_o^\omega)\sin(\Theta_o^\omega + \Theta_g^{2\omega})}, \end{aligned} \tag{A.3}$$

where $\Theta_g^{2\omega}$ is the angle of refraction ot the 2ω wave in the glass and $n_s^{2\omega}$ is the indice of refraction of the slab at the second harmonic frequency. The 2ω wave generated in the glass undergoes linear refraction at the glass/air interface to give rise to the s and p final SHG intensity. The corresponding linear Fresnel coefficients $f_s^{2\omega}$ and $f_p^{2\omega}$ are given by [39]

$$\begin{aligned} f_s^{2\omega} &= \frac{2\sin\Theta_t^{2\omega}\cos\Theta_g^{2\omega}}{\sin(\Theta_g^{2\omega} + \Theta_t^{2\omega})}, \\ f_p^{2\omega} &= \frac{2\sin\Theta_t^{2\omega}\cos\Theta_g^{2\omega}}{\sin(\Theta_g^{2\omega} + \Theta_t^{2\omega})\cos(\Theta_g^{2\omega} - \Theta_t^{2\omega})}, \end{aligned} \tag{A.4}$$

where $\Theta_t^{2\omega}$ is the external angle of refraction for the 2ω wave. Moreover, the requirement of the necessary condition of continuity for the tangential electric and magnetic fields at each interface [35] leads to an additional relation between the different angles of refraction

$$\sin\Theta_t^{2\omega} = n_g^{2\omega}\sin\Theta_g^{2\omega} = n_s^\omega \sin\Theta_s^\omega = \sin\Theta_o^\omega. \tag{A.5}$$

Eqs. (A.1)–(A.5) were used conjointly in order to simulate the polarization dependence of the SHG intensity given by Eq. (3) according to the fitting procedure explained in the text.

Appendix B

As first done by Heinz et al. [21] the nonlinear susceptibility of a molecular monolayer can be

measured by calibration of the SHG intensity against a quartz plate. Indeed, using the Maker fringe method [40] on an Y-cut quartz plate turned around its optical axis, and whose thickness is much greater than the coherence length L_c of the crystal, the maximum intensity $I_{max}^{2\omega}$ which is expected at nearly normal incidence with respect to a p-polarized pump of intensity I_p^{ω} can be approximated by the following tractable formula [41]:

$$I_{max}^{2\omega} = \frac{128\pi\omega^2\chi_{11q}^2 T_p^{2\omega}(T_p^{\omega})^2 L_c^2 (I_p^{\omega})^2}{c^3 (n_q^{\omega})^2 n_q^{2\omega}}, \qquad \text{(B.1)}$$

In the above equation, χ_{11q} is the first component of the volume nonlinear susceptibility tensor of quartz, $n_q^{\omega} = 1.534$ and $n_q^{2\omega} = 1.547$ its ordinary indices at wavelengths $\lambda^{\omega} = 1064$ nm and $\lambda^{2\omega} = 532$ nm of the Nd:YAG laser, and $L_c = \lambda^{\omega}/4(n_q^{2\omega} - n_q^{\omega}) = 20.6$ μm. T_p^{ω} and $T_p^{2\omega}$ are the transmission factors of the input and output plate interfaces for the waves at, respectively, ω and 2ω. These factors reduce to the well-known Fresnel factor $((n_q^{\omega,2\omega} - 1)/(n_q^{\omega,2\omega} + 1))^2$ for normal incidence and emergence of the waves. Then using the same intensity and p-polarization for the ingoing light sent to monolayers and to quartz so as to measure SHG intensities, the χ_{15} coefficient of the monolayers can be straightforwardly found from the ratio of Eq. (3) over Eq. (B.1).

References

[1] M. Zochowski, M. Wachowiak, C.X. Falk, L.B. Cohen, Y.W. Lam, S. Antic, D. Zecevic, Biol. Bull. 198 (1) (2000) 1.
[2] D.A. Dombeck, M. Blanchard-Desce, W.W. Webb, J. Neurosci. 24 (2004) 999.
[3] A.C. Millard, L. Jin, A. Lewis, L.M. Loew, Opt. Lett. 28 (2003) 1121.
[4] A.C. Millard, L. Jin, M.-de Wei, J.P. Wuskell, A. Lewis, L.M. Loew, Biophys. J. 86 (2004) 11169.
[5] L.O. Sandre, S. Charpak, M. Blanchard-Desce, J. Mertz, Biophys. J. 80 (2001) 1568.
[6] E. Fluhler, V.G. Burnham, L.M. Loew, Biochemistry 24 (1992) 5749.
[7] L.M. Loew, L.B. Cohen, J. Dix, E. Fluhler, V. Montana, G. Salama, J.Y. Wu, J. Membr. Biol. 130 (1992) 1.
[8] S. Rohr, B.M. Salzberg, Biophys. J. 67 (1994) 1301.
[9] J. Zhang, R.M. Davidson, M.-de Wei, L.M. Loew, Biophys. J. 74 (1998) 48.
[10] T. Pons, L. Moreaux, O. Mongin, M. Blanchard-Desce, J. Mertz, J. Biomed. Opt. 8 (2003) 428.
[11] V. Alain, M. Blanchard-Desce, I. Ledoux, J. Zyss, Chem. Commun. (2000) 353.
[12] M. Blanchard-Desce, C. R. Physique 3 (2002) 439.
[13] J.L. Oudar, J. Chem. Phys. 67 (1977) 446.
[14] J.L. Oudar, D.S. Chemla, J. Chem. Phys. 66 (1977) 2664.
[15] K. Clays, A. Persoons, Phys. Rev. Lett. 66 (1991) 2980.
[16] D. Laage, W.H. Thompson, M. Blanchard-Desce, J.T. Hynes, J. Phys. Chem. A (2003) 6032.
[17] O.F.J. Noordman, N.F. van Hultst, Chem. Phys. Lett. (1996) 145.
[18] G. Olbrechts, R. Strobbe, K. Clays, A. Persoons, Rev. Sc. Instrum. 69 (1998) 2233.
[19] M.C. Flipse, R. de Jonge, R.H. Woudenberg, A.W. Marsman, C.A. van Walree, L.W. Jenneskens, Chem. Phys. Lett. 245 (1995) 297.
[20] C.K. Chen, T.F. Heinz, D. Ricard, Y.R. Shen, Phys. Rev. Lett. 46 (1981) 1010.
[21] T.F. Heinz, H.W.K. Tom, Y.R. Shen, Phys. Rev. A 28 (1983) 1883.
[22] Th. Raising, Y.R. Shen, Phys. Rev. Lett. 55 (1985) 2903.
[23] R.M. Corn, D.A. Higgins, Chem. Rev. 94 (1994) 107.
[24] B. Dick, A. Gierulski, G. Marowsky, G.A. Reider, Appl. Phys. B 38 (1995) 107.
[25] G.J. Simpson, S.G. Westerbuhr, K.L. Rowlen, Anal. Chem. 72 (2000) 887.
[26] L. Moreaux, T. Pons, V. Dambrin, M. Blanchard-Desce, J. Mertz, Opt. Lett. (2003) 625.
[27] A. Yariv, P. Yeh, in: Optical Waves in Crystals, Wiley, New York, 1984.
[28] A. Leray, L. Leroy, Y. Le Grand, C. Odin, A. Renault, V. Vié, D. Rouède, T. Mallegol, O. Mongin, M.H.V. Werts, M. Blanchard-Desce, Langmuir 20 (2004) 8165.
[29] G.J. Simpson, K.L. Rowlen, J. Am. Chem. Soc. 121 (1999) 2635.
[30] O. Mongin, T. Mallegol, M. Blanchard-Desce, to be published.
[31] W.H. Press, S.A. Teukolsky, W.T. Vetterling, B.P. Flannery, Numerical Recipies in Fortran 77: The Art of Scientific Computing, Cambridge University Press, Cambridge, 2001, p. 402.
[32] Y.R. Shen, The Principles of Non-linear Optics, Wiley, New York, 1992.
[33] E.W. Weisstein, in: CRC Concise Encyclopedia of Mathematics, Chapman & Hall/CRC, London, 1999, p. 953.
[34] J. Zyss, I. Ledoux, J.F. Nicoud, in: J. Zyss (Ed.), Molecular Nonlinear Optics, Academic Press, New York, 1994 (Chapter 4).
[35] N. Bloembergen, P.S. Pershan, Phys. Rev. 128 (1962) 606.
[36] T.F. Heinz, in: H.E. Ponath, G.I. Stegeman (Eds.), Nonlinear Surface Electromagnetic Phenomena, 1991 (Chapter 5).
[37] V. Mizrahi, J.E. Sipe, J. Opt. Soc. Am. B 5 (1988) 660.

[38] C. Flueraru, S. Schrader, V. Zauls, B. Dietzel, H. Motschmann, Opt. Commun. 182 (2000) 457.
[39] M. Born, E. Wolf, Principles of Optics, third ed., Pergamon Press, Oxford, 1993, p. 40.
[40] P.D. Maker, R.W.M. Nisenhoff, C.M. Savage, Phys. Rev. Lett. 8 (1962) 121.
[41] J. Jerphagnon, S.K. Kurtz, J. Appl. Phys. 41 (1970) 1667.